

Investigation of open volume in photochromic YH_xO_y thin films by positron annihilation lifetime spectroscopy

Ziying Wu^{1,*}, Tom de Krom¹, Gijs van Hattem¹, Giorgio Colombi², Bernard Dam², Henk Schut¹, Marcel Dickmann³, Werner Egger³, Christoph Hugenschmidt⁴, and Stephan W.H. Eijt¹

¹*Department of Radiation Science and Technology, Faculty of Applied Sciences, Delft University of Technology, Delft, The Netherlands*

²*Materials for Energy Conversion and Storage, Department of Chemical Engineering, Faculty of Applied Sciences, Delft University of Technology, Delft, The Netherlands*

³*Institut für angewandte Physik und Messtechnik, Bundeswehr Universität München, Germany*

⁴*Physics Department and Heinz Maier-Leibnitz Zentrum (MLZ), TU München, Germany*



REACTOR
INSTITUTE
DELFT



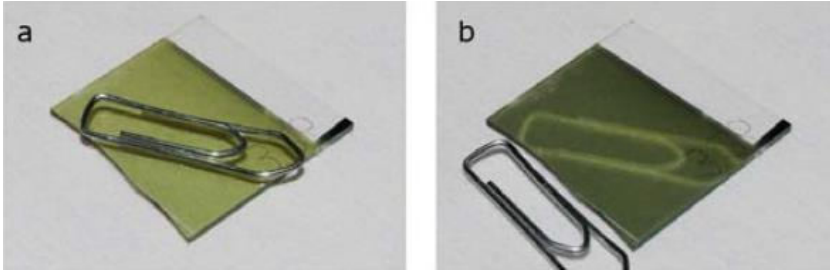
der Bundeswehr
Universität München



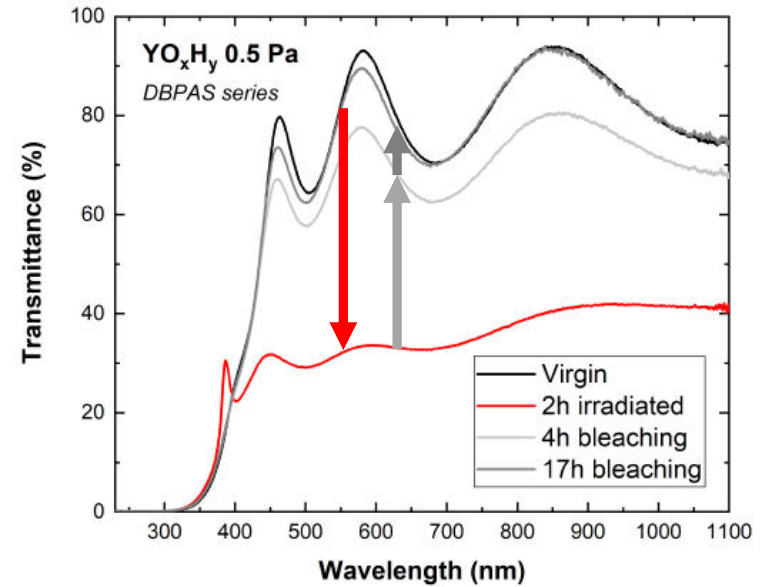
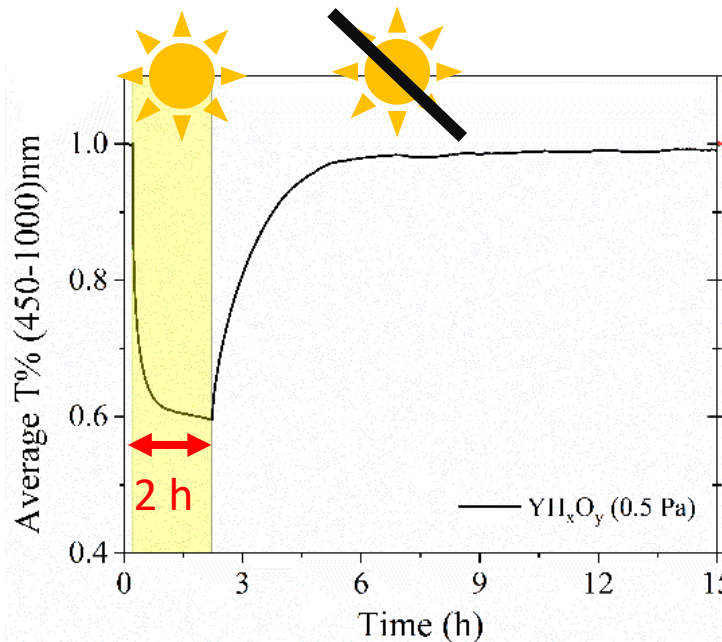
contents

- Introduction: photochromic YH_xO_y thin films
- Vacancies and nanopores in YH_xO_y and Y, $YH_{\sim 2}$, Y_2O_3 studied by PALS
- Nanostructural changes in YH_xO_y thin films upon illumination studied by *in-situ* DB-PAS
- Conclusions

Photochromic YH_xO_y thin films



Picture: T. Mongstad *et al.* "A new thin film photochromic material: Oxygen-containing yttrium hydride", *Sol. Energy Mat. Solar Cells* (2011)

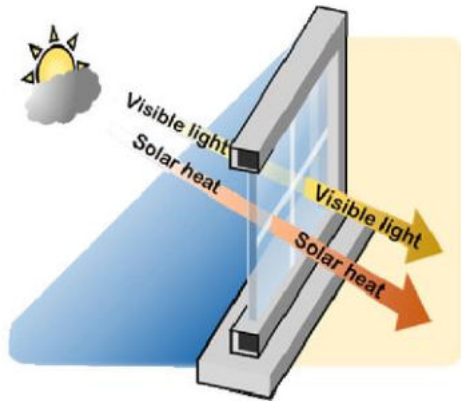


Picture: S.W.H. Eijt *et al.* "Photochromic YO_xH_y Thin Films Examined by in situ Positron Annihilation Spectroscopy", *ACTA PHYS POL A* (2020)

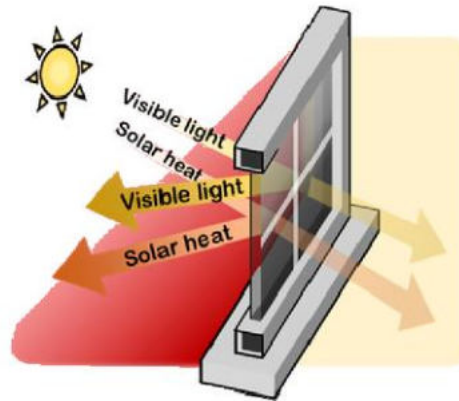
Photo-darkening:
Reduced sub-bandgap transmission

Bleaching: nearly full recovery

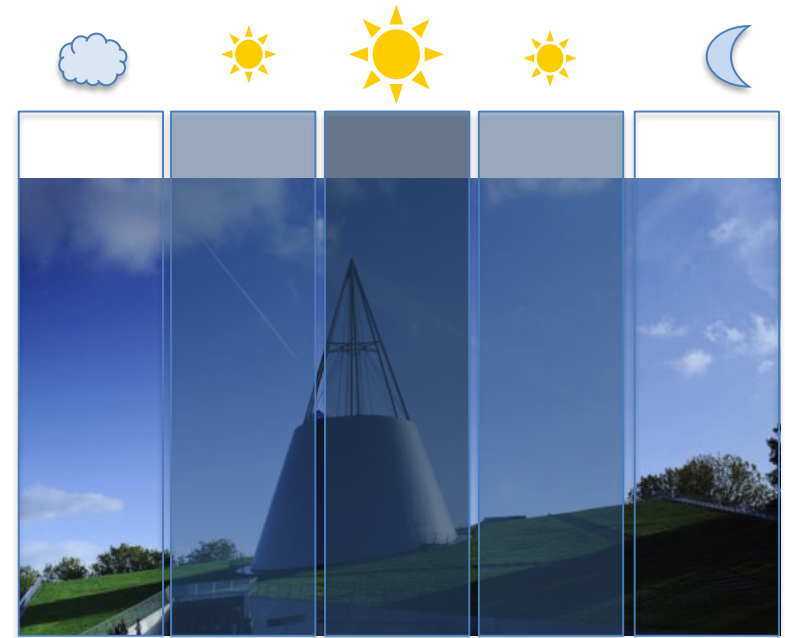
Smart windows for energy-saving



Transparent
Weak sunlight



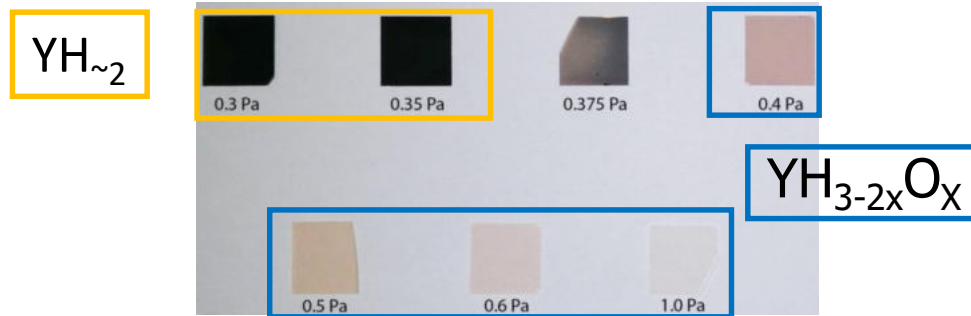
Opaque
Strong sunlight



Picture: Proc. SPIE 10555, Emerging Liquid Crystal Technologies XIII, 1055516 (2018)

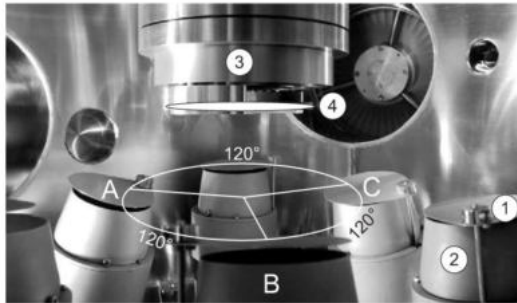
Synthesis of YH_xO_y thin films

Sputtered $\text{YH}_{\sim 2}$ films (300-500 nm) $\xrightarrow{\text{Oxidized in air}}$ photochromic YH_xO_y films

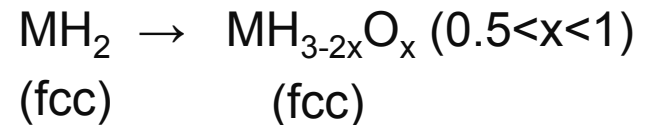
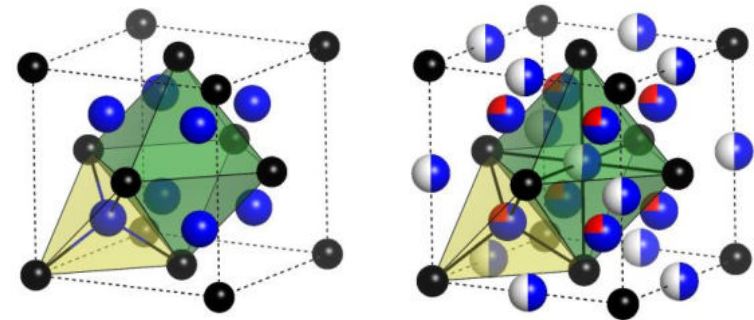


Color changes

Metal-to-semiconductor change

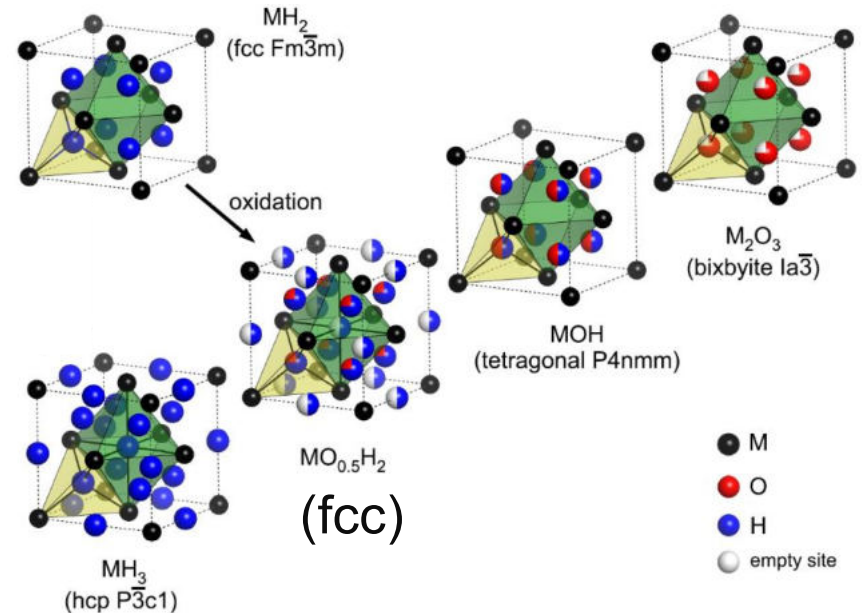
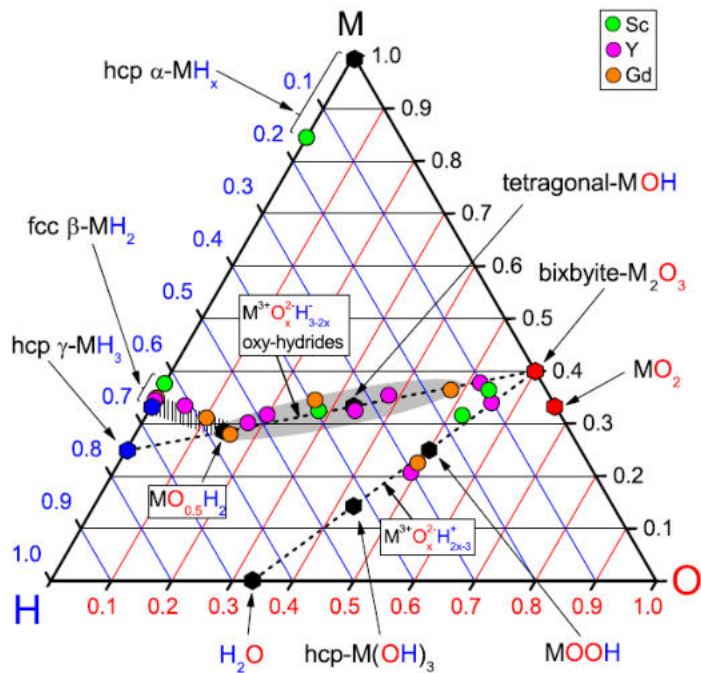


Reactive magnetron sputtering



Phase diagram of YH_xO_y thin films

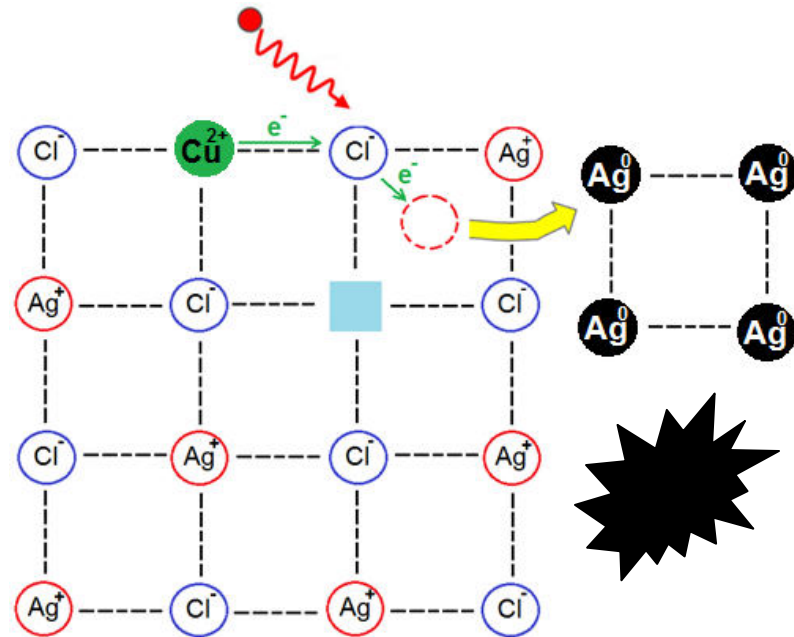
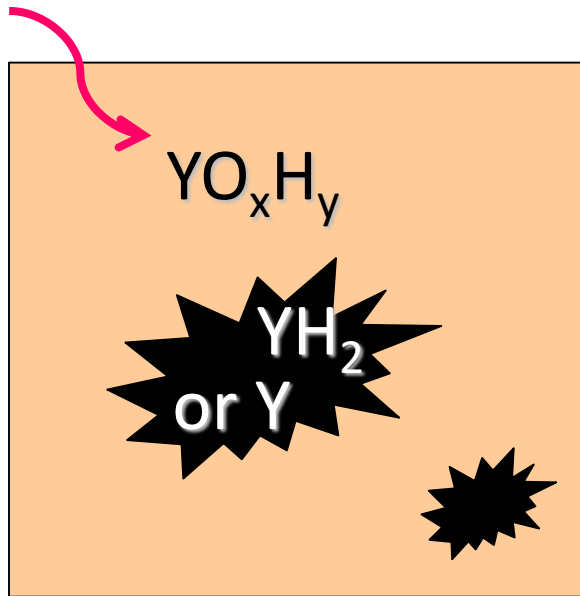
Pictures: Cornelius et al., J. Phys. Chem. Lett. 10 (2019) 1342–1348



Grey area ($MH_{3-2x}O_x$): photochromic

Why are these films photochromic?

Mechanism: similar to Ag-based photochromism?

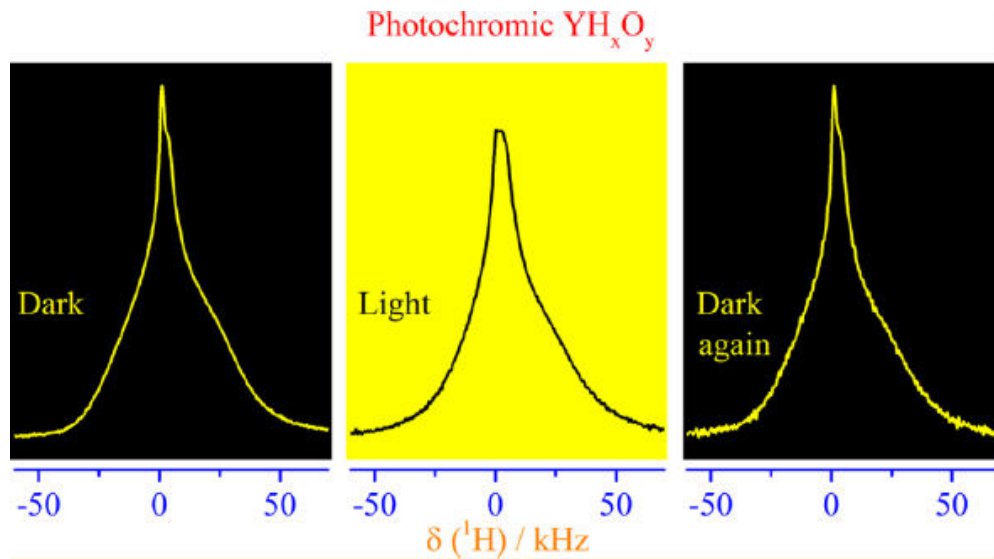


Pictures: F. Nafezarefi, doctoral thesis, TU Delft, 2020

Yttrium (dihydride) domains growth?

Photochromic Cu^+ doped $AgCl$ glass:
formation of Ag metal clusters

Mechanism: Role of Hydrogen?

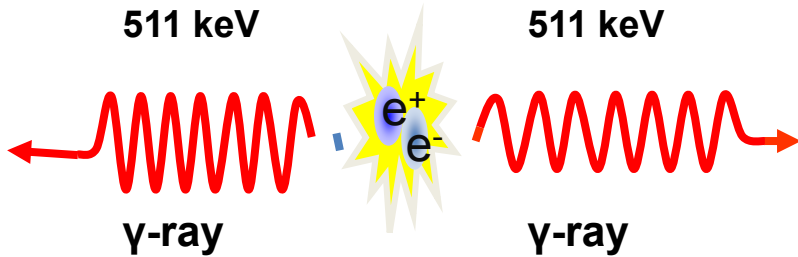


Picture: **C. Vinod Chandran *et al.*** "Solid-State NMR Studies of the Photochromic Effects of Thin Films of Oxygen-Containing Yttrium Hydride", *J. Phys. Chem. C* 118 (2014) 22935 - 22942

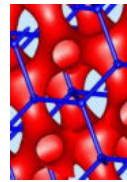
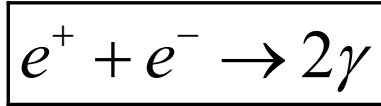
NMR:

- mobile hydrogen 'disappears' upon UV illumination
- reversible!

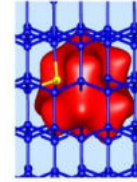
Positron annihilation spectroscopy



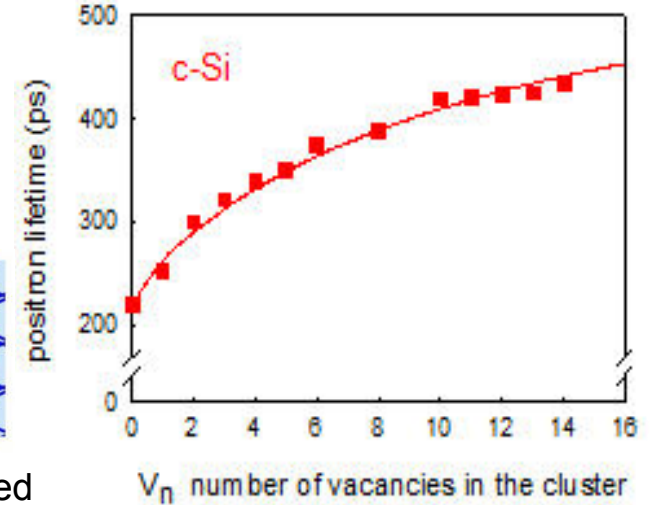
Annihilation: creation of 2 γ -rays (most common process)



lattice



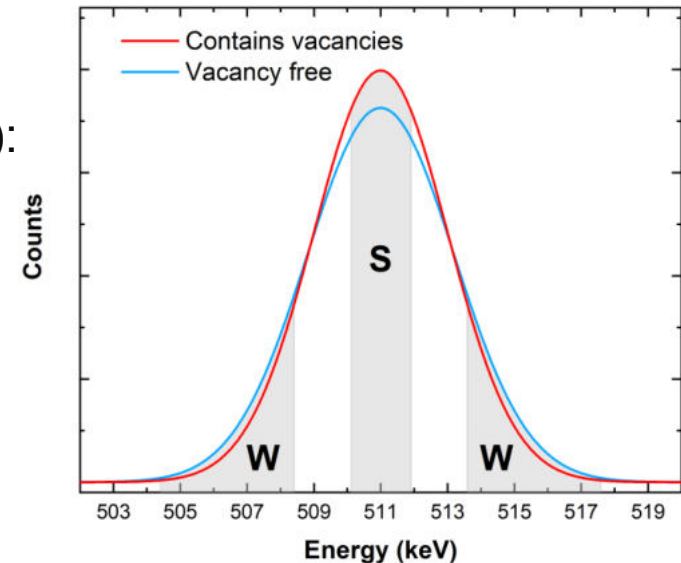
e^+ trapped at vacancy



- Positron Annihilation Lifetime Spectroscopy (PALS):
the size and concentration of vacancies

- Doppler Broadening Positron Annihilation Spectroscopy (DB-PAS):

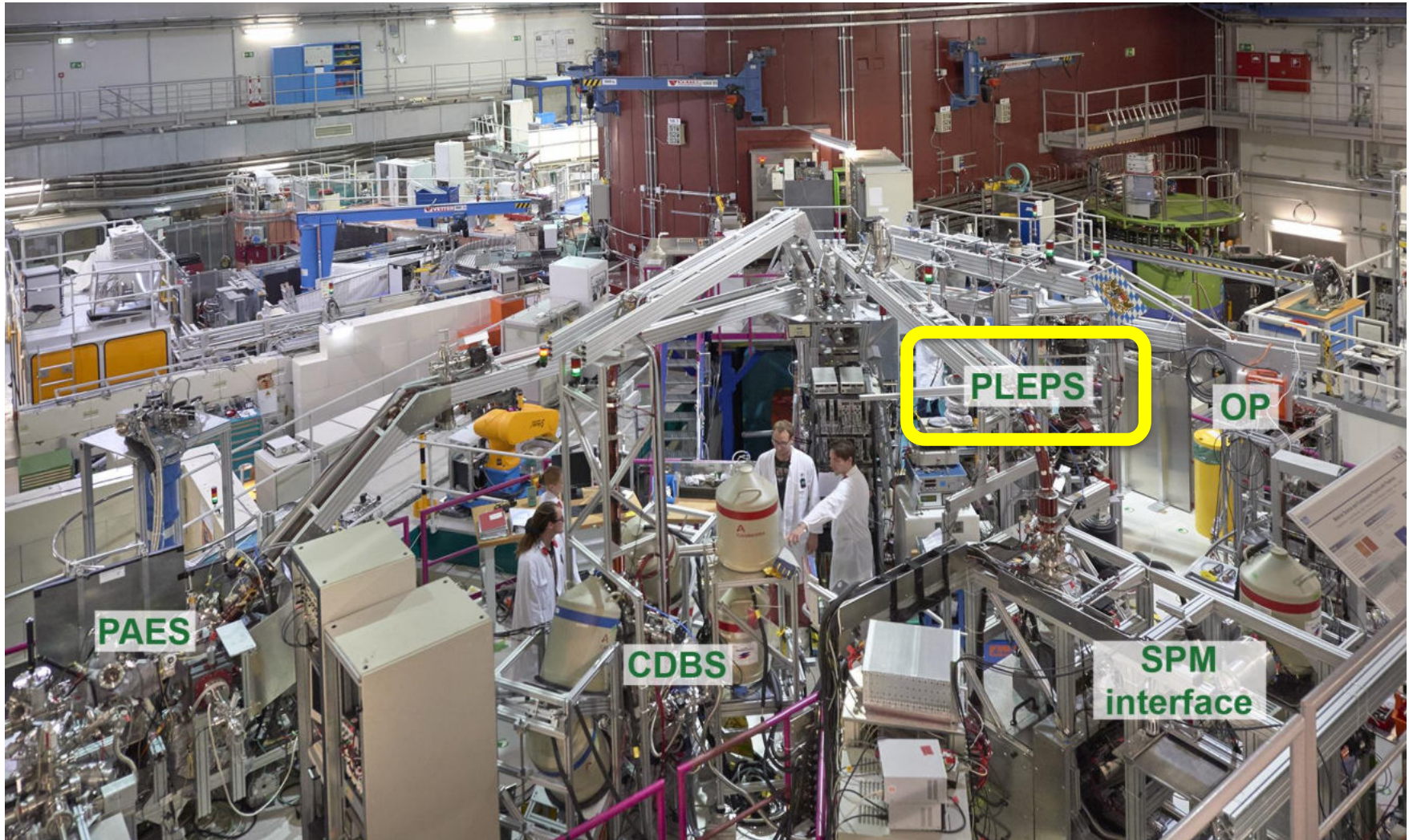
Vacancies
electronic structure



Motivations:

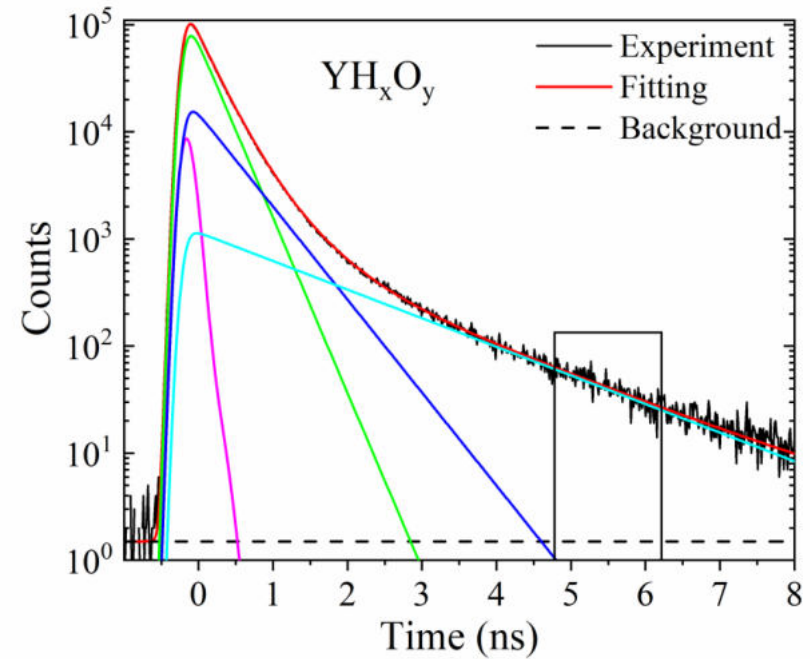
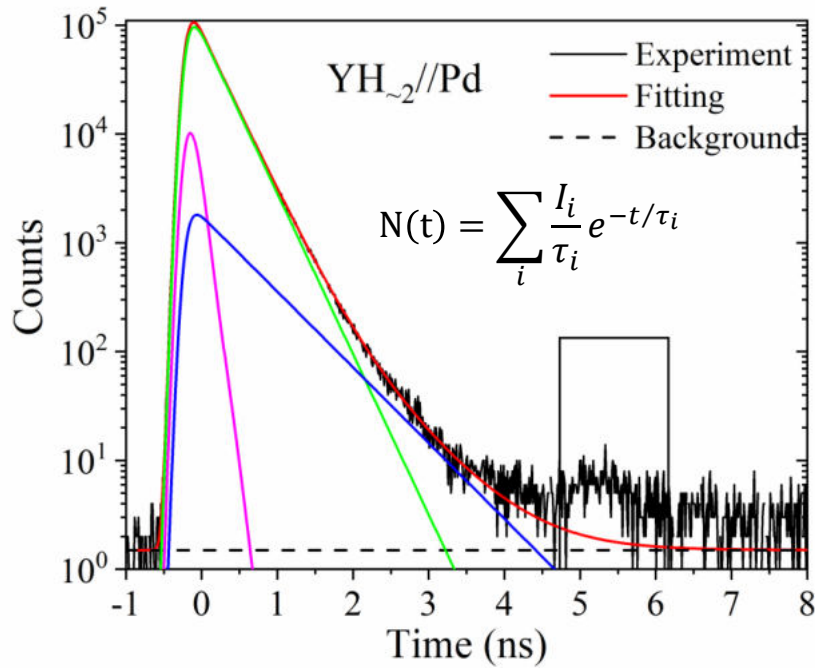
- What are the sizes and concentrations of vacancies in as-deposited YH_xO_y and Y, $YH_{\sim 2}$, Y_2O_3 ? ----- by PALS
- The variation of electronic structure----- by DB-PAS
- Do vacancies and electronic structure change upon illumination? Its relationship with photochromic effect?
----- by in-situ DB-PAS

PALS @ MLZ Garching



The open volume in YH_xO_y and Y, YH_2 , Y_2O_3 by PALS

Positron lifetime spectra @ 4 keV POSWIN analysis



YH_{~2}:

τ_1 : 65 ± 3 ps

τ_2 : 279 ± 1 ps I_2 : 92 ± 0.2

τ_3 : 683 ± 22 ps

YH_xO_y:

τ_1 : 47 ± 5 ps

τ_2 : 266 ± 4 ps I_2 : 71 ± 2

τ_3 : 500 ± 20 ps I_3 : 22 ± 2

τ_4 : 1.63 ± 0.03 ns

Two-defect trapping model [2]

For extracting the bulk lifetime (τ_b), positron trapping rate (k_{di}), and defect concentrations (C_i).

Main equations of this two-defect trapping model:

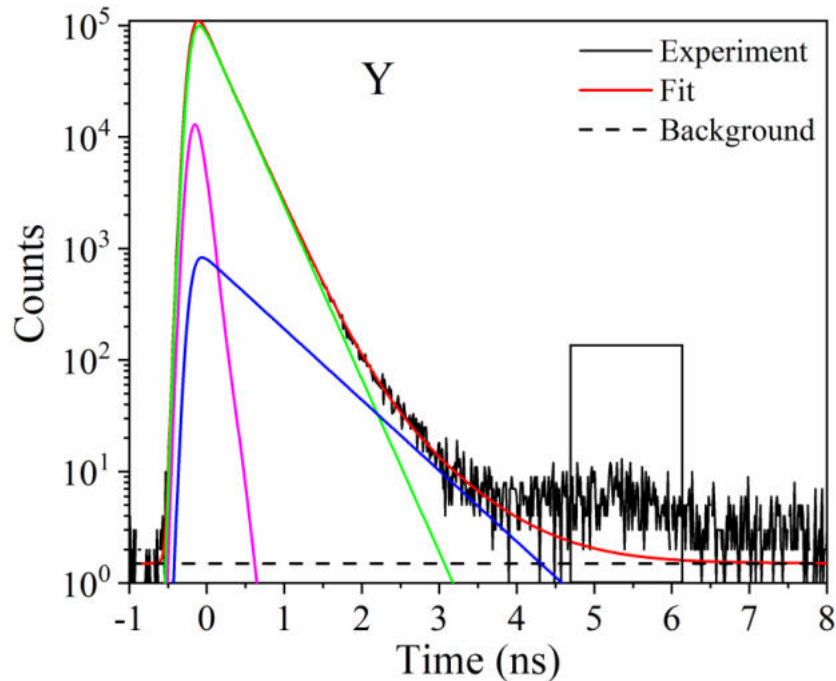
$$k_{d1} = \mu C_1 = I_2 \left(\frac{1}{\tau_1} - \frac{1}{\tau_2} \right)$$

$$k_{d2} = \mu C_2 = I_3 \left(\frac{1}{\tau_1} - \frac{1}{\tau_3} \right)$$

$$\tau_b^{cal.} = \left(\frac{I_1}{\tau_1} + \frac{I_2}{\tau_2} + \frac{I_3}{\tau_3} \right)^{-1}$$

Assuming $\mu = 10^{15} s^{-1}$

The open volume in YH_xO_y and Y, YH_2 , Y_2O_3 by PALS



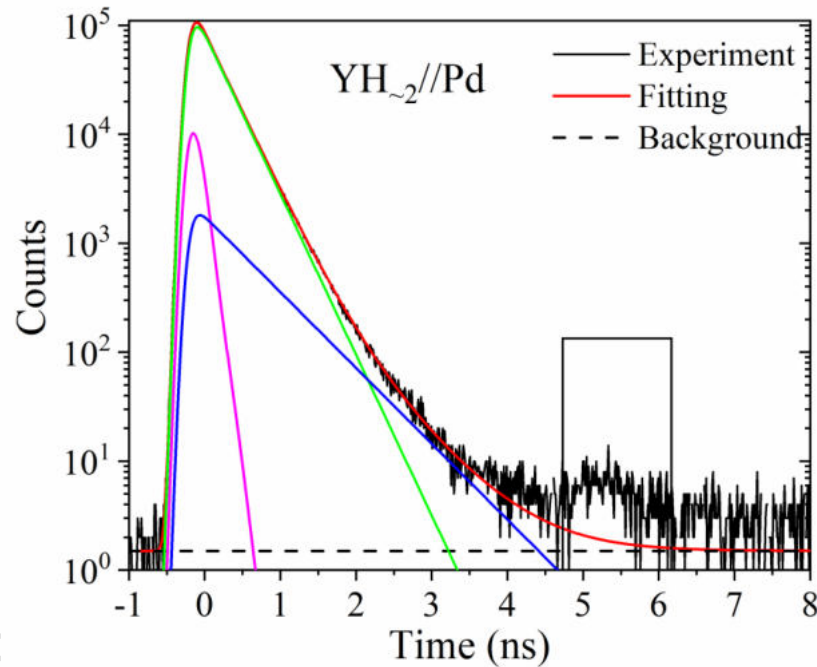
- Y thin film:

τ_b : ~ 235 ps, not far away from $\tau_b^{\text{exp.}}$ (249 ps) and $\tau_b^{\text{cal.}}$ (215 ps) [3]

τ_2 : 279 ps, increases $\sim 19\%$ compare to τ_b , **V_Y mono-vacancy**;

I_2 : 92%, concentration $\sim 1.0 \times 10^{-5}$.

The open volume in YH_xO_y and Y, YH_2 , Y_2O_3 by PALS

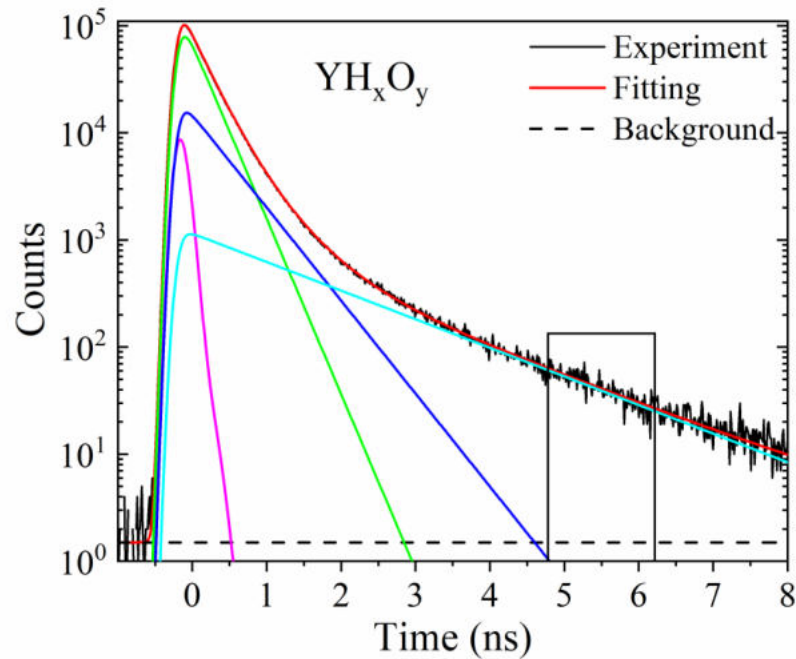


- $YH_2//Pd$ thin film:

τ_b : ~ 260 ps, increase $\sim 10\%$ compare to τ_b (Y), due to the increase of the volume per unit cell ($\sim 6\%$), XRD.

τ_2 : 294 ps, increases $\sim 14\%$ compare to τ_b , V_Y mono-vacancies;
 I_2 : 91%, concentration $\sim 0.8 \times 10^{-5}$.

The open volume in YH_xO_y and Y, YH_2 , Y_2O_3 by PALS



YO_xH_y (0.5 Pa):

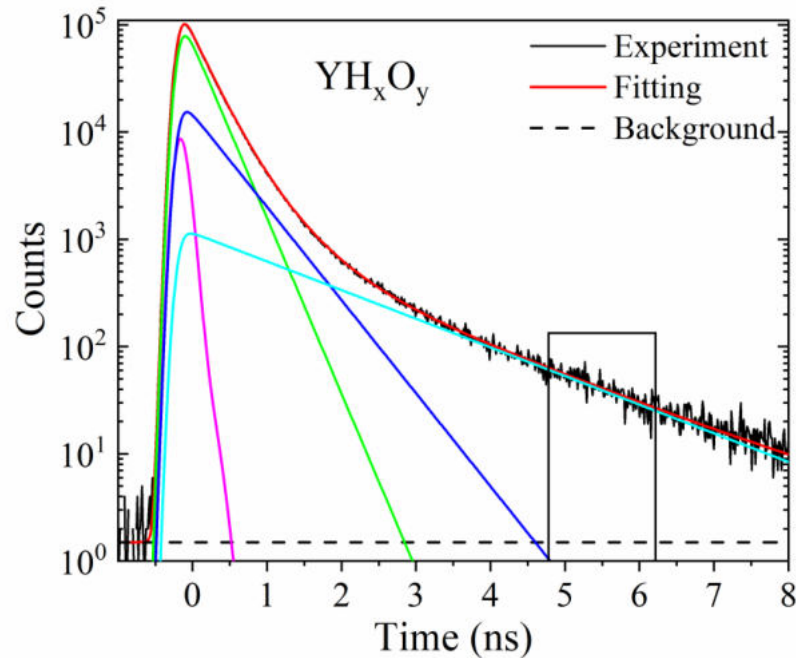
τ_b : ~220 ps

τ_2 : 266 ps, increases ~19% compare to τ_b , **V_Y mono-vacancies**, I_2 : 71%, $C_{\text{defect } 1} \sim 1.5 \times 10^{-5}$.

τ_3 : 500 ps, **vacancy clusters**, I_3 : 22%, $C_{\text{defect } 2} \sim 0.5 \times 10^{-5}$.

τ_4 : ~1.6 ns, **o-Ps formation**: presence of nanovoids

The open volume in YH_xO_y and Y, YH_2 , Y_2O_3 by PALS



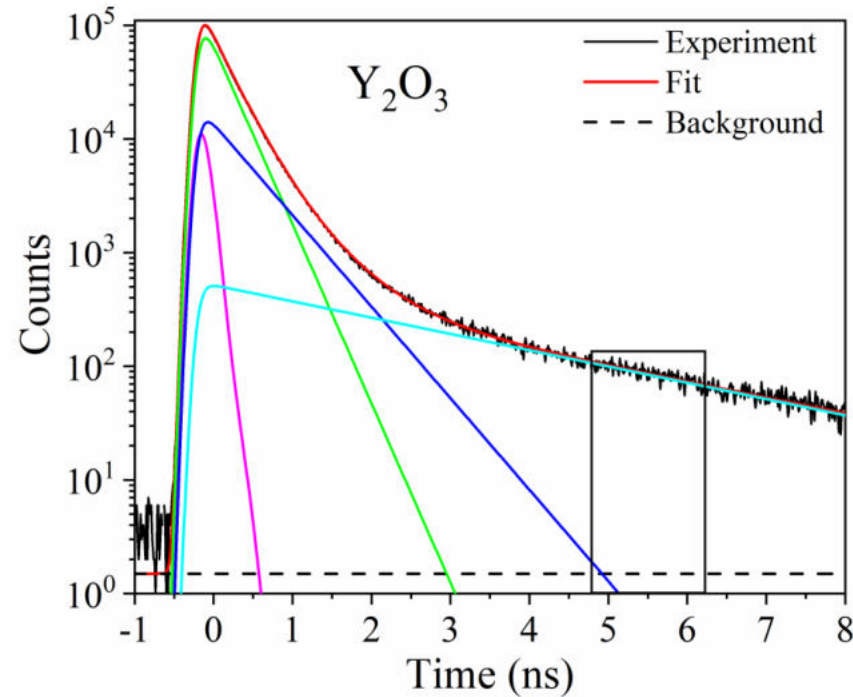
YO_xH_y (0.5 Pa):

τ_3 : 500 ps, **vacancy clusters**, $>V_5$ e.g. in GeSn and P doped Ge, $\tau \sim 450$ ps, $V_{>5}$ [7,8]

τ_4 : ~ 1.6 ns, **o-Ps formation**: presence of nanovoids, radius ~ 0.25 nm, according to the Tao-Eldrup (TE) model [5,6]; assuming spherical pores, ~ 7 atoms missing in one unit cell of YH_xO_y ($\sim V_7$).

V_7 clusters could be responsible for both τ_3 and τ_4

The open volume in YH_xO_y and Y, YH_2 , Y_2O_3 by PALS



Y_2O_3 thin film (0.3 Pa):

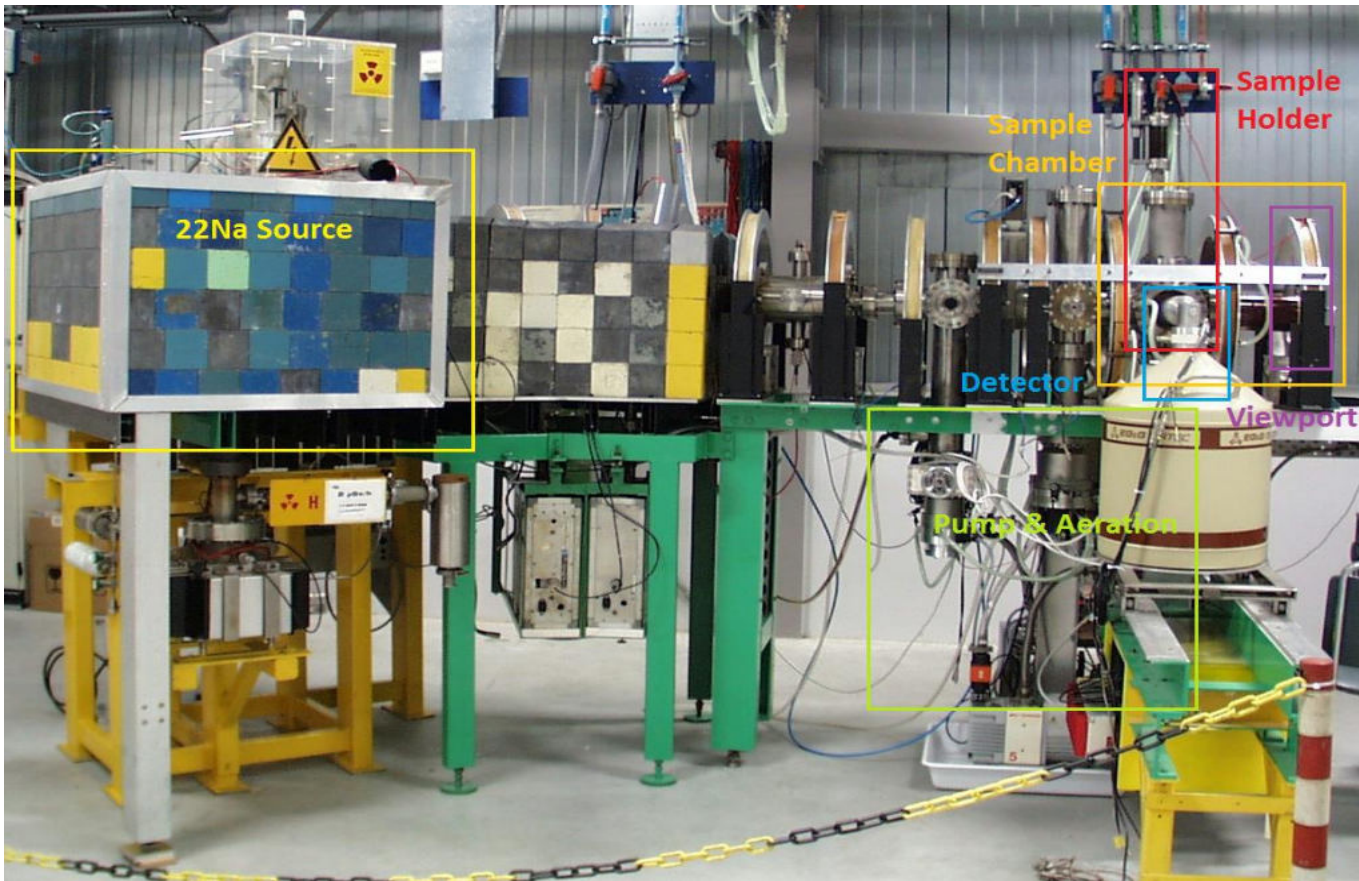
τ_b : ~237 ps, close to 239 ps for Y_2O_3 powder [9]

τ_2 : 276 ps, V_Y mono-vacancy, $C_{\text{defect } 1} \sim 0.9 \times 10^{-5}$.

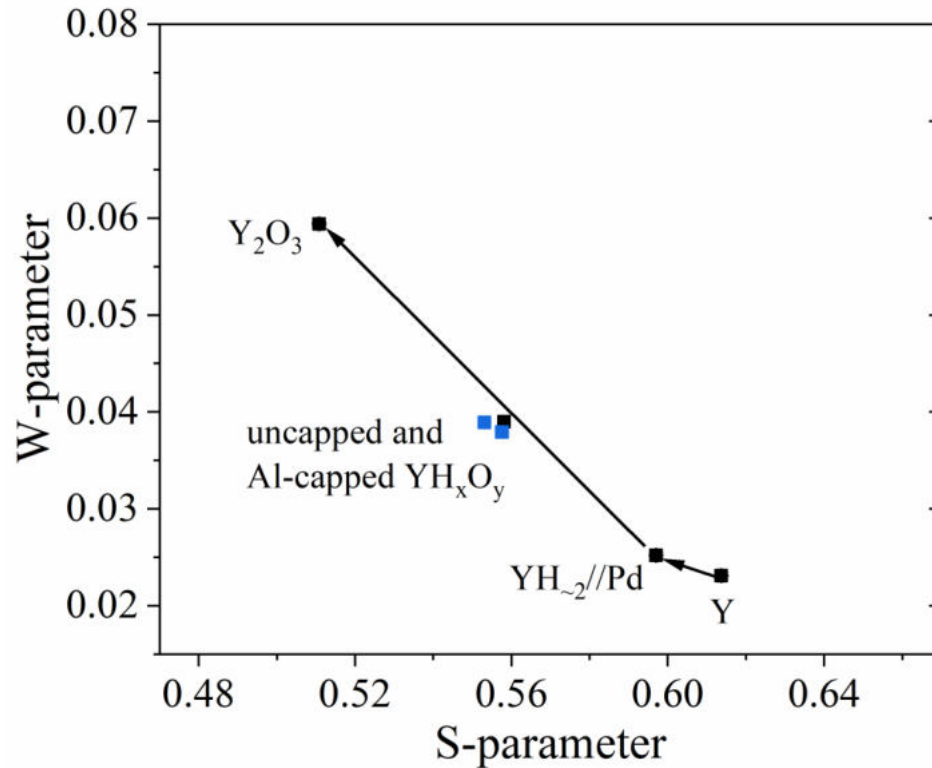
τ_3 : 539 ps, vacancy clusters, $C_{\text{defect } 2} \sim 0.3 \times 10^{-5}$.

τ_4 : ~3 ns, o-Ps formation in nanovoids, radius ~0.37 nm^[5,6], $\sim V_{14}$

Doppler Broadening Positron Annihilation Spectroscopy @ TU Delft

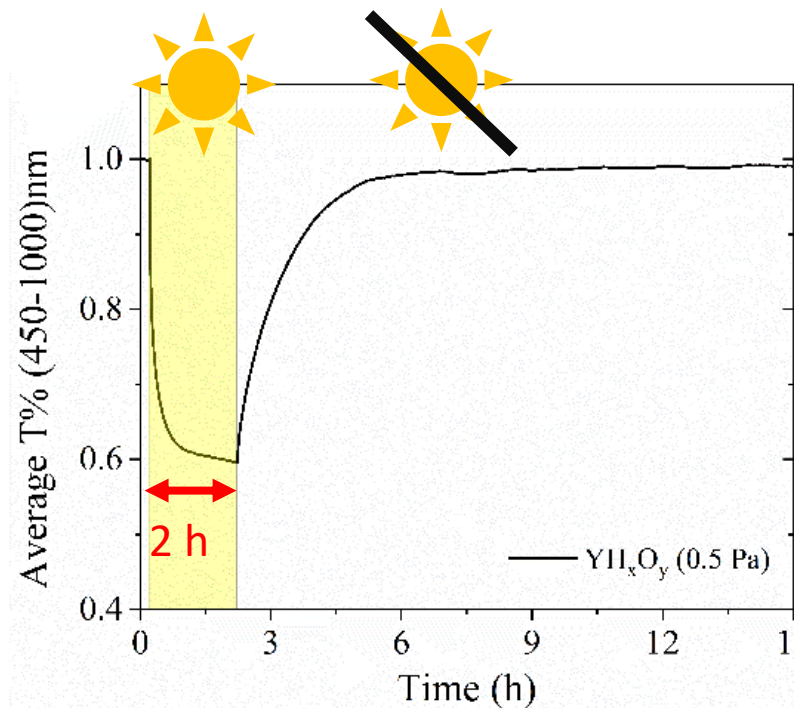
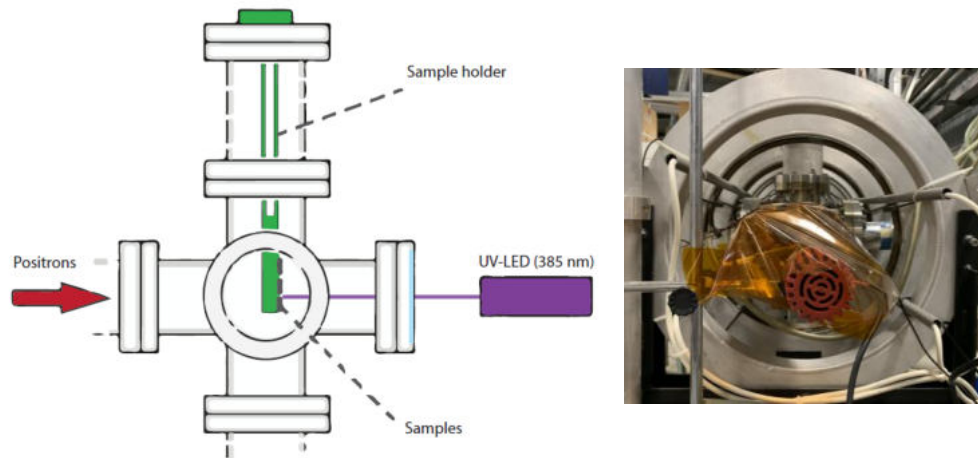


DB-PAS studies of as-deposited YH_xO_y and Y, $\text{YH}_{\sim 2}$, Y_2O_3 films



- Y: narrow electronic momentum distribution
- $\text{YH}_{\sim 2}$: more localized valence electronic orbitals due to metal-H bonds
- Y_2O_3 : insulating, strong localized valence electrons of O atoms
- YH_xO_y : semiconducting, intermediate electron momentum distribution

In-situ illumination DB-PAS studies of YH_xO_y films

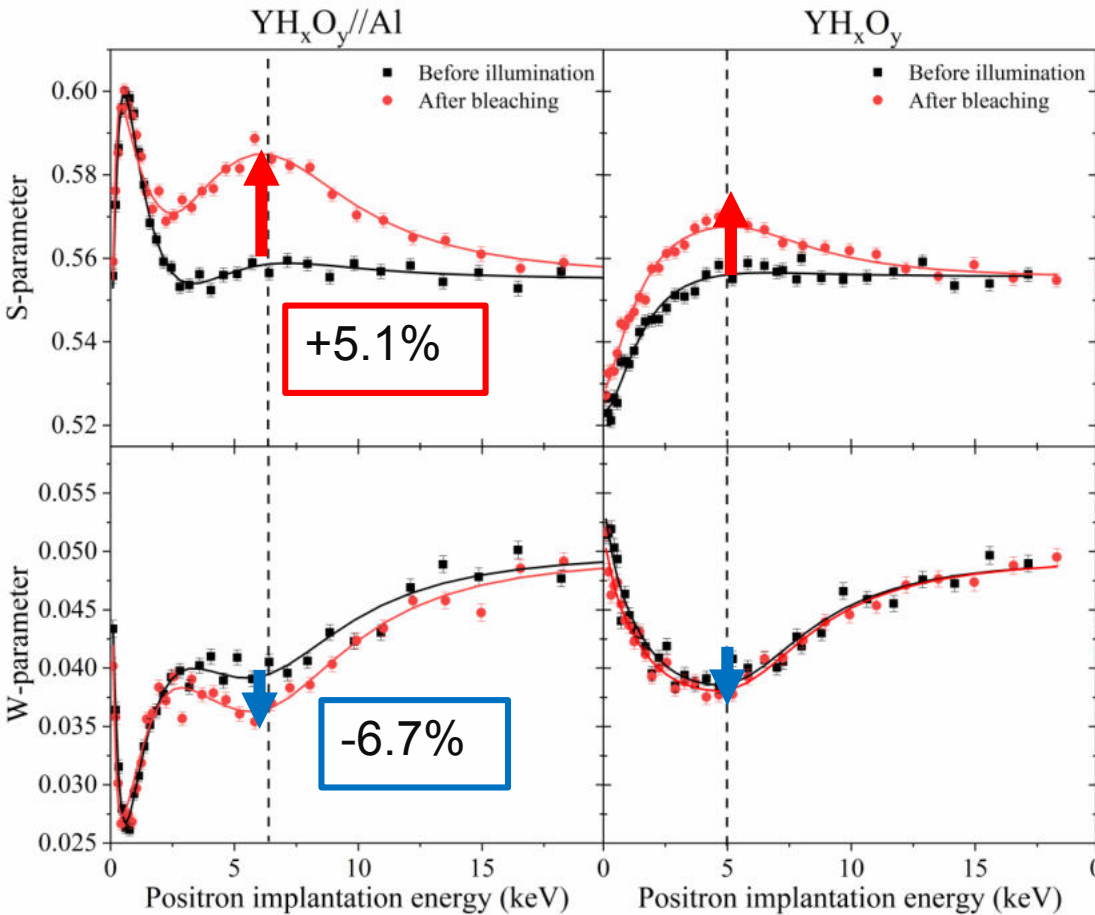


Transmittance fully recovers

In-situ illumination DB-PAS

(after ~2.5 h illumination + ~38 h bleaching)

S & W not fully recover



S increases and W decreases permanently

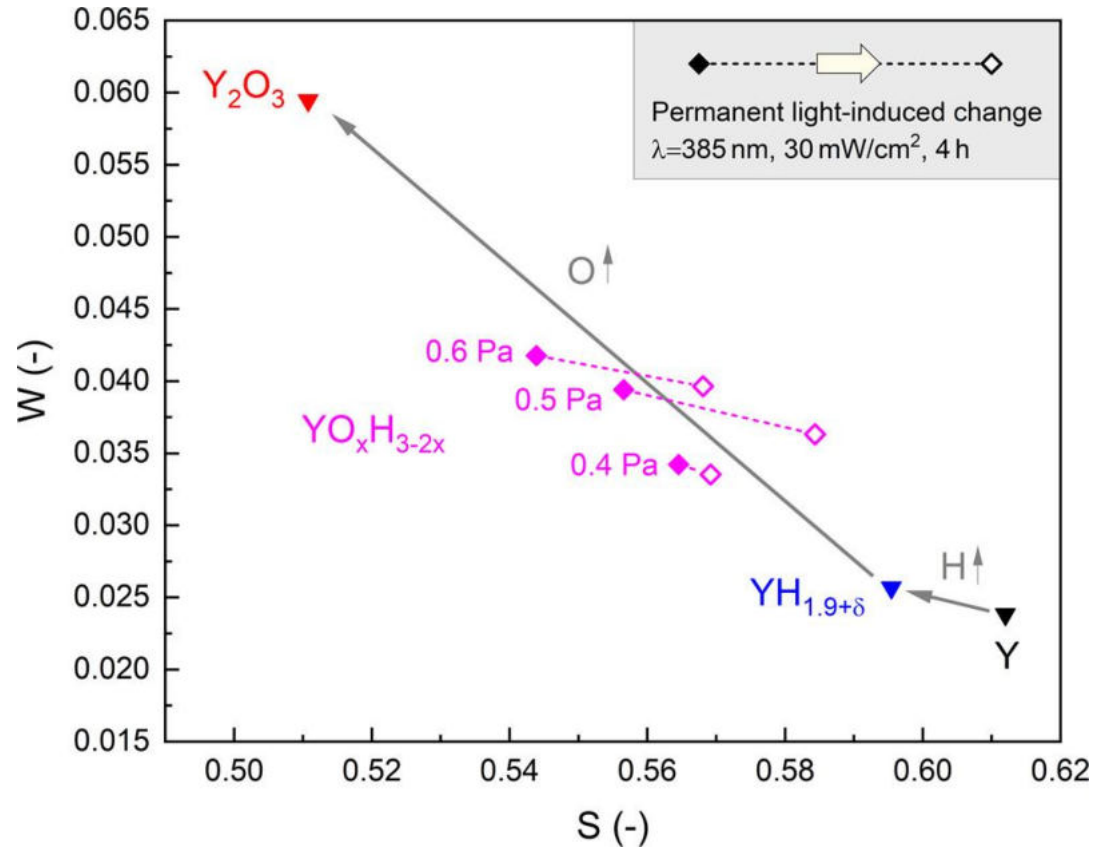
excluded: V_Y cation vacancies (near-saturation trapping of e^+ in V_Y seen by PALS)

Likely small vacancy clusters: V_Y-V_H , V_H-V_H , V_O-V_H di-vacancies

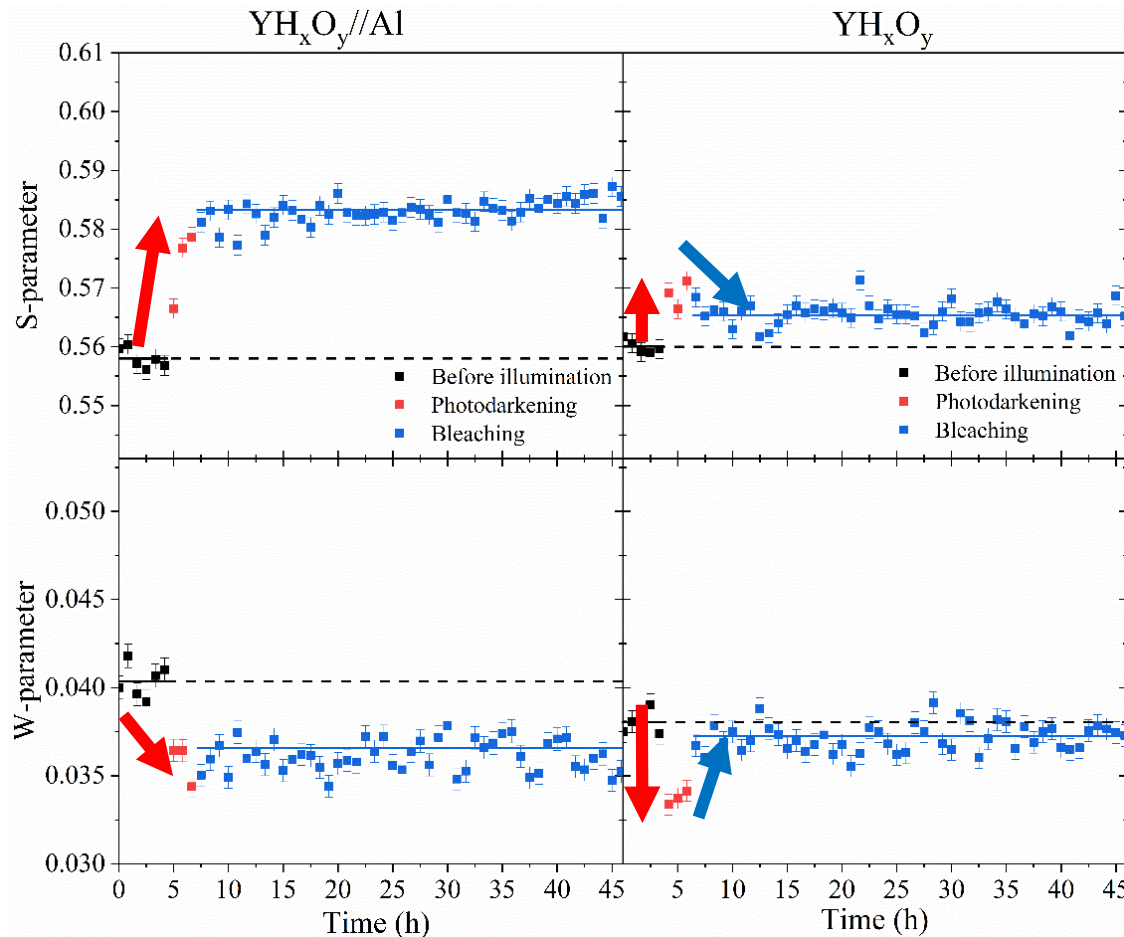
Anion mobility during illumination

In-situ illumination S-W map of Al capped YH_xO_y films

Right figure: G. Colombi et al., *ACS Photonics* 8 (2021) 709–715



Time-dependence DB-PAS under illumination



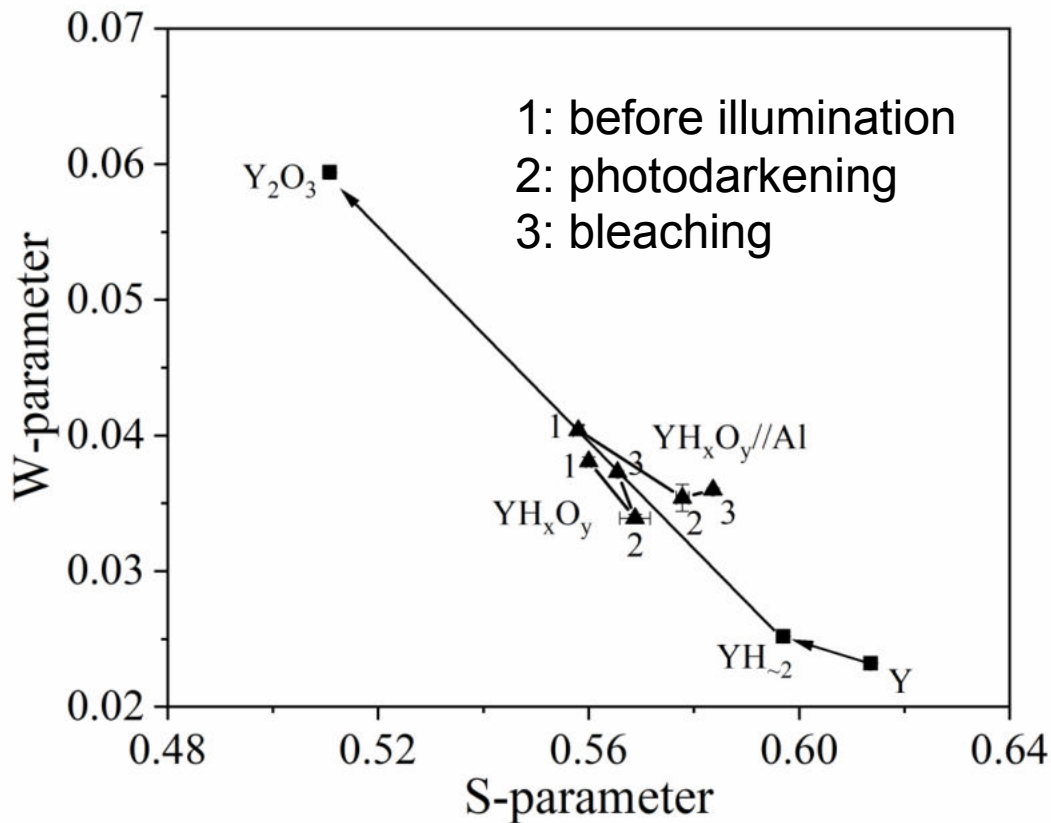
- Permanent changes after bleaching: formation of small vacancy clusters
- Larger changes of S/W during illumination



a second type of nanostructural changes

- GdH_xO_y : Similar behaviour

In-situ illumination S-W map of YH_xO_y films



$$R = \frac{\Delta S}{\Delta W}$$

$$R(\text{oxide} \rightarrow \text{hydride}) \approx -2.5$$

YH_xO_y//Al:

- $R(1 \rightarrow 2) \approx -4$
- irreversible formation of di-vacancies/small vacancy clusters

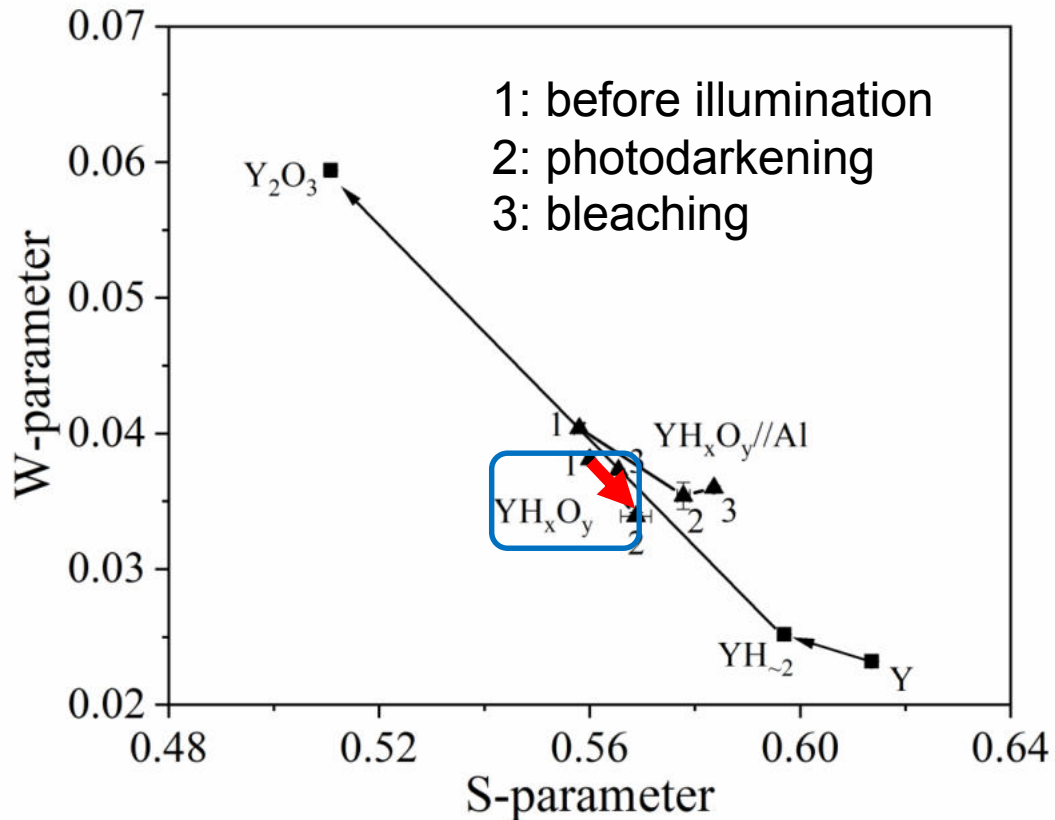
YH_xO_y:

- $R(1 \rightarrow 2) \approx -2$, Similar to $R(\text{oxide} \rightarrow \text{hydride})$, S-W shifts to the hydride direction



Partially reversible formation of domains with low O:H ratio

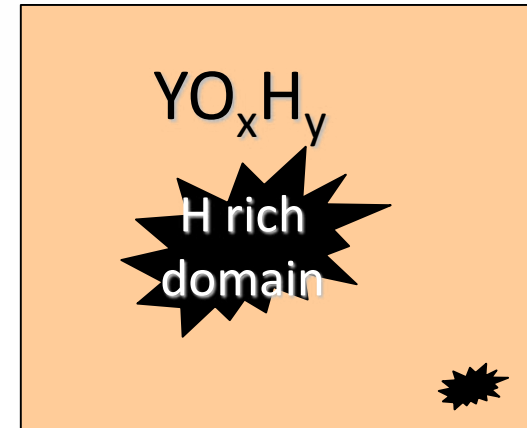
In-situ illumination S-W map of YH_xO_y films



Local composition YH_2O_x ($x < 0.5$), $Y^{3+} \rightarrow Y^{2+}$

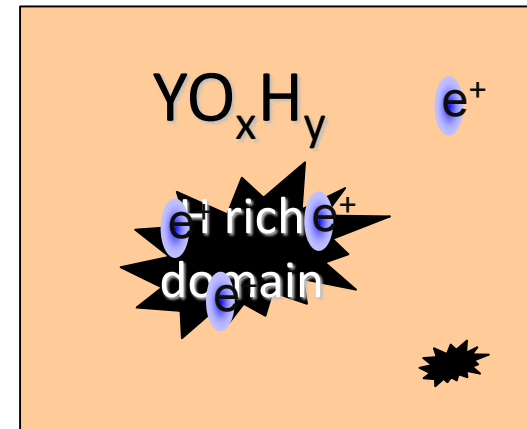
metallic-like H-rich domains along with mobility of H

e^+ preferentially trap in H-rich domains (e^+ affinity)



Conclusions

1. Mono-vacancies dominant Y and $\text{YH}_{\sim 2}$ films at a concentration of $\sim 10^{-5}$ per Y atom, while in addition vacancy clusters and nanopores are found in YH_xO_y and Y_2O_3 .
2. Variation in electronic structure of metal, metal hydride, semiconducting oxyhydride and insulating oxide.
3. In-situ illumination DB-PAS on YH_xO_y films:
 - permanent formation of small vacancy clusters;
 - partially reversible formation of H-rich domains along with the mobility of H.



Acknowledgement:



Tom de Krom, Gijs van Hattem, Henk Schut, Ekkes Brück and Stephan W.H. Eijt



Giorgio Colombi, Diana Chaykina, and Bernard Dam,



Marcel Dickmann, Werner Egger



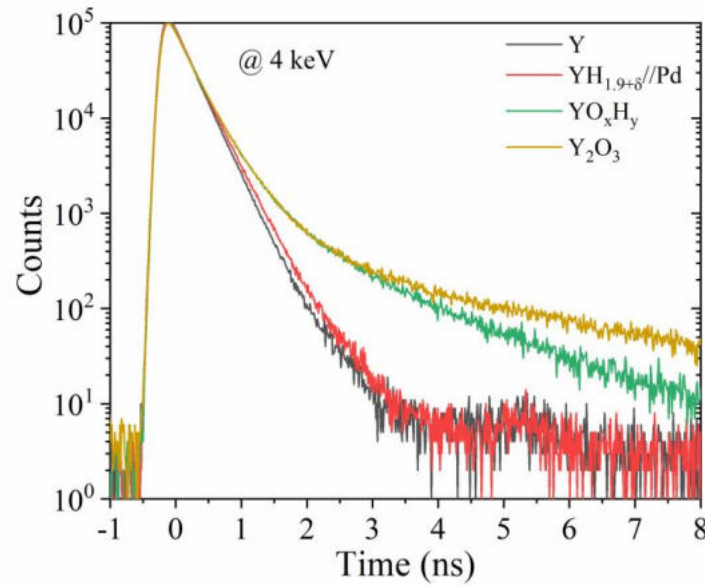
Christoph Hugenschmidt



Thanks for your attention!



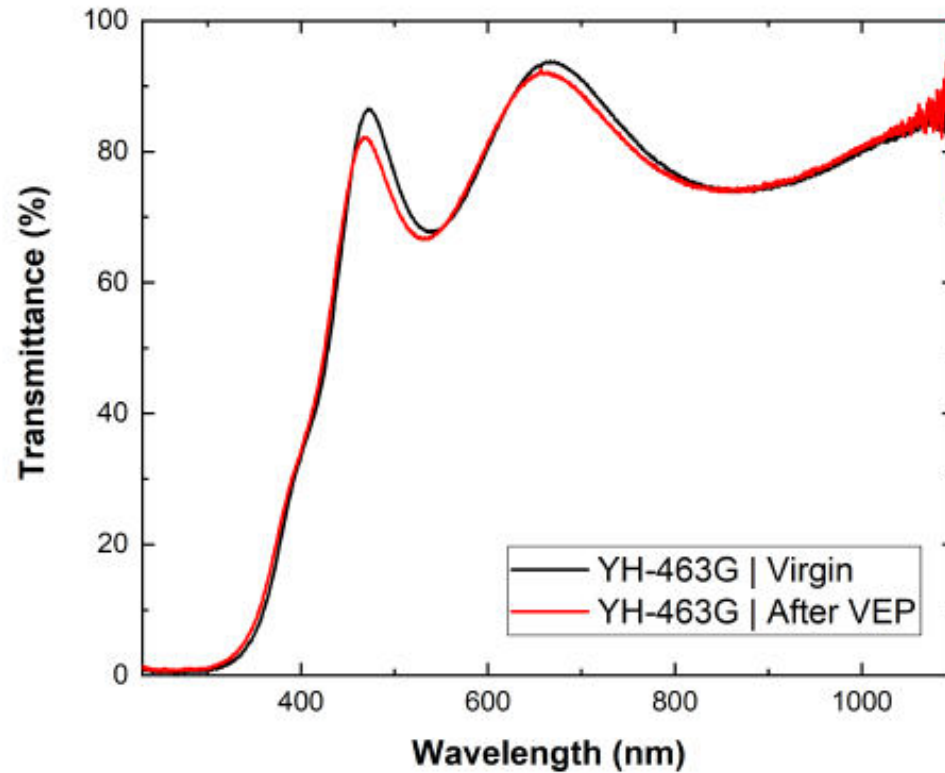
PALS



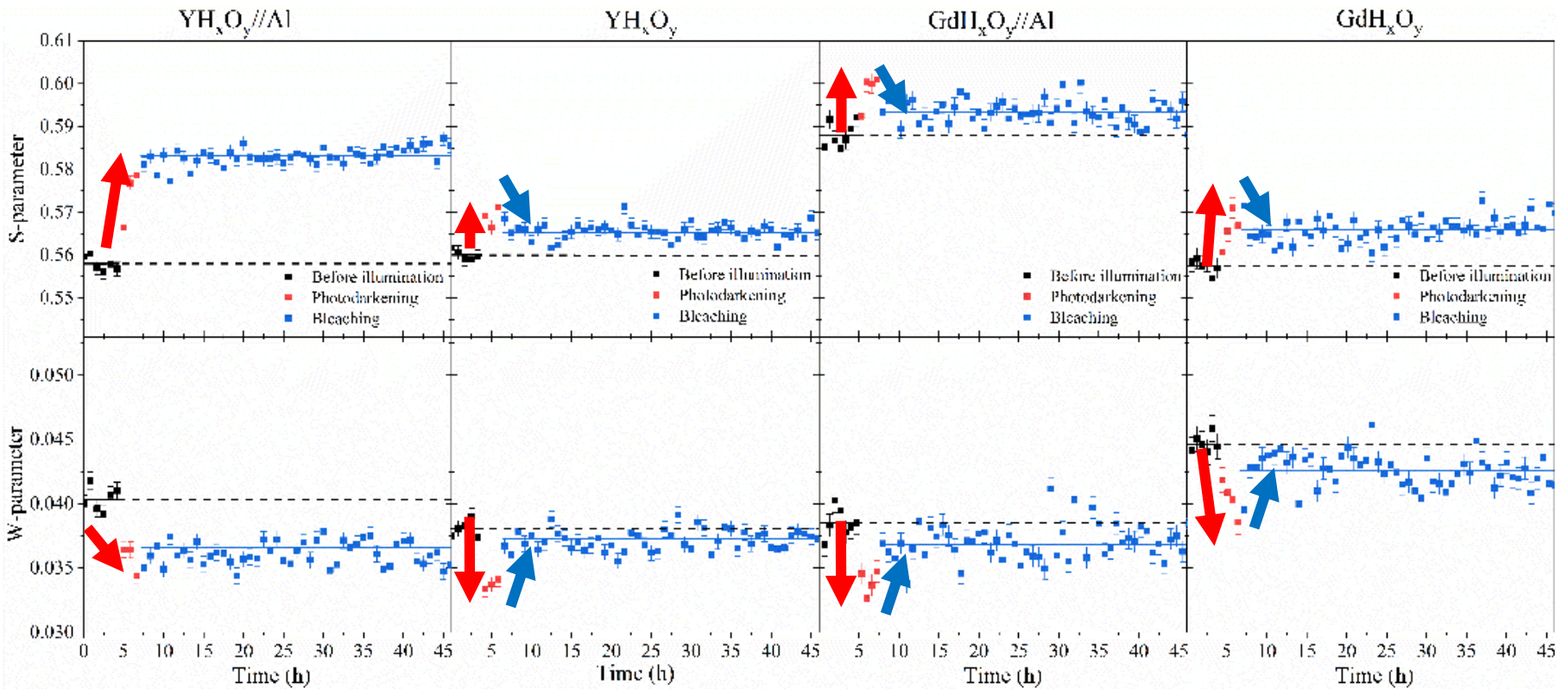
Thin films	τ_1 (ps)	τ_2 (ps)	τ_3 (ps)	τ_4 (ns)	I_1 (%)	I_2 (%)	I_3 (%)	I_4 (%)	τ_{av} (ps)
Y	65±3	279±1	683±22	-	6±0.2	92±0.2	1.5±0.2	-	272±1
YH _{~2} //Pd	73±5	294±1	624±17	-	5±0.2	92±0.2	3±0.3	-	293±3
YH _x O _y	47±5	266±4	500±20	1.63±0.03	3.8±0.2	71±2	22±2	4.2±0.2	365±17
Y ₂ O ₃	58±5	276±4	539±16	3.03±0.06	5.1±0.3	71±2	21±2	3.4±0.1	412±13

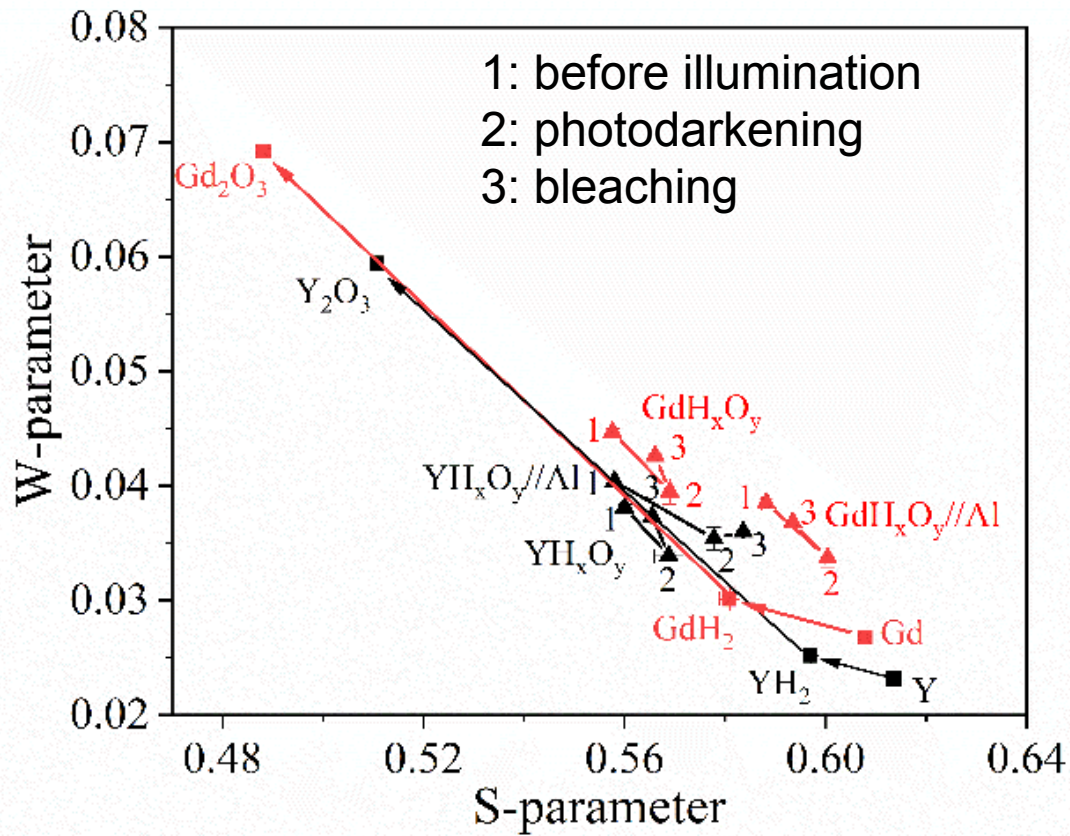
Samples	τ_b (ps)	k_1 (10^{10} s^{-1})	k_2 (10^{10} s^{-1})	C_1 (10^{-5})	C_2 (10^{-5})
Y	235±4	1.0±0.1	0.02±0.001	1.0±0.1	0.02±0.001
YH _{~2} //Pd	260±6	0.8±0.1	0.03±0.003	0.8±0.1	0.03±0.003
YH _x O _y -1	218±11	1.5±0.3	0.5±0.1	1.5±0.3	0.5±0.1
YH _x O _y -2	224±9	1.2±0.2	0.33±0.05	1.2±0.2	0.33±0.05
Y ₂ O ₃	237±9	0.9±0.1	0.27±0.03	0.9±0.1	0.27±0.03

Transmittance before VEP and after VEP



Time-dependence DB-PAS under illumination

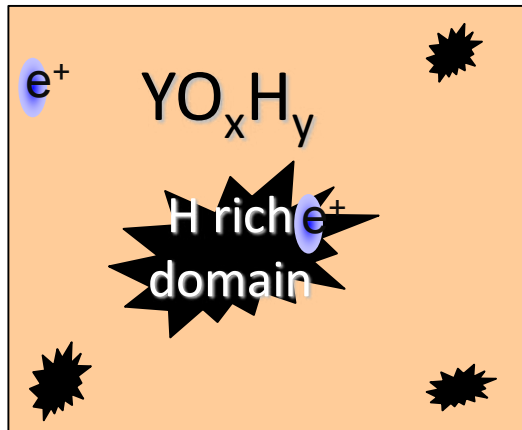




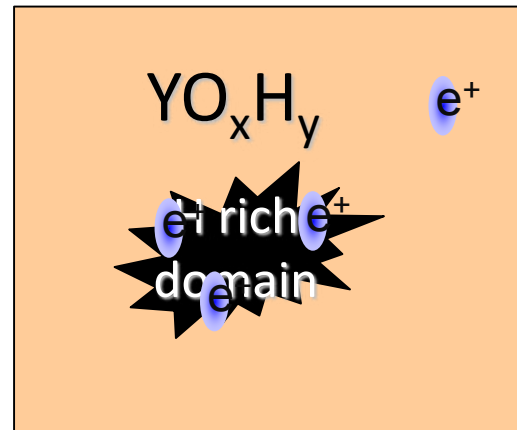
In-situ illumination S-W map of YH_xO_y films

❖ W: -12% during illumination with only ~6 vol. % metallic domains

High concentration of metallic domains? W -12%



High fraction of positron annihilate in the clusters



The trapping fraction of Li in MgO is ~92% with Li only occupy 3 vol.% with radius of 3-7 nm [M.A. van Huis et al., 2002 PRB].

Diffusion-limited trapping model [10,11]:

The fraction of positron annihilate in H-rich domain:

$$f_{clusters} = \frac{\kappa}{\kappa + \lambda_{bulk}} = \frac{4\pi r D_+ c}{4\pi r D_+ c + \lambda_{bulk}}$$

$$L_+ = \sqrt{D_+ \tau}$$

κ is the positron trapping rate in clusters (s^{-1})
 λ_{bulk} is the annihilation rate in oxyhydride (s^{-1})
 r is the radius of the cluster (m)
 c is the concentration of clusters (m^{-3})
 D_+ is the diffusion coefficient ($m^2 s^{-1}$)
 L_+ is the diffusion length (m)
 τ is the positron lifetime (s)

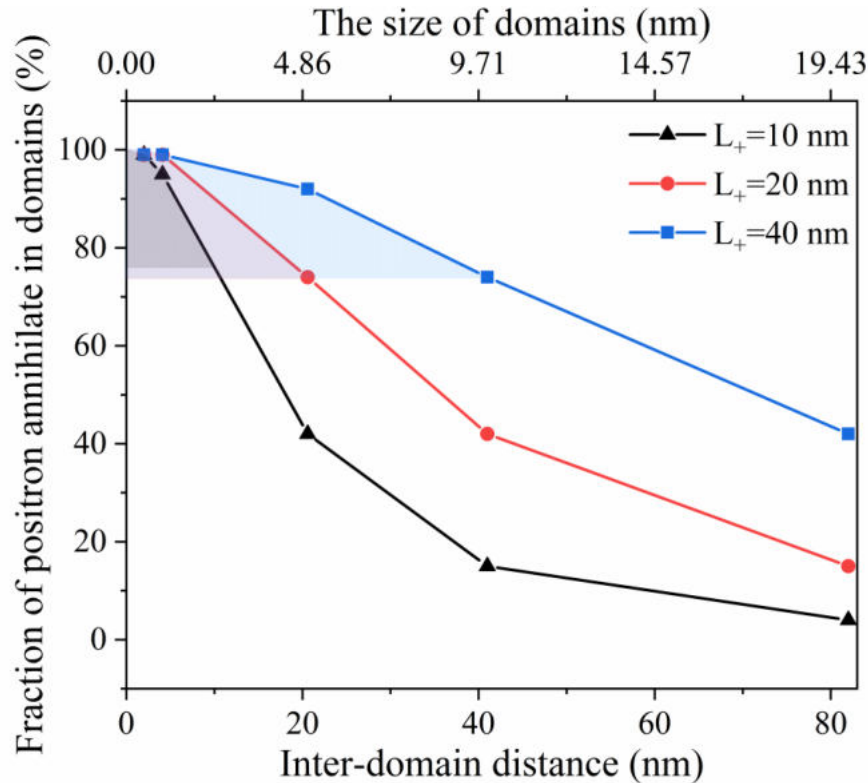
On the condition that:

- The difference in e^+ affinity is sufficient large (several tenths of eV)

Assumptions:

- The clusters are spherical and homogeneous distribute in bulk.
- De-trapping of e^+ from H-rich domains is neglected.

Diffusion-limited trapping model



Experimental L_+ is between 10-40 nm from VEPFIT

- ~6 vol. % H-rich domains dominate >70% positron signal
- The average size of domains is ~1 to ~10 nm.